NASA/TM-2010-216387

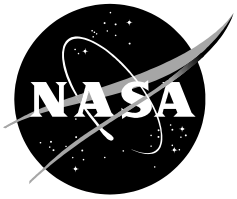

Application of Approximate Unsteady Aerodynamics for Flutter Analysis

Chan-gi Pak and Wesley W. Li
NASA Dryden Flight Research Center
Edwards, California

July 2010

NASA STI Program…in Profile

Since its founding, NASA has been dedicated to the advancement of aeronautics and space science. The NASA scientific and technical information (STI) program plays a key part in helping NASA maintain this important role.

The NASA STI program operates under the auspices of the Agency Chief Information Officer. It collects, organizes, provides for archiving, and disseminates NASA's STI. The NASA STI program provides access to the NASA Aeronautics and Space Database and its public interface, the NASA Technical Report Server, thus providing one of the largest collections of aeronautical and space science STI in the world. Results are published in both non-NASA channels and by NASA in the NASA STI Report Series, which includes the following report types:

- TECHNICAL PUBLICATION. Reports of completed research or a major significant phase of research that present the results of NASA Programs and include extensive data or theoretical analysis. Includes compilations of significant scientific and technical data and information deemed to be of continuing reference value. NASA counterpart of peer-reviewed formal professional papers but has less stringent limitations on manuscript length and extent of graphic presentations.

- TECHNICAL MEMORANDUM. Scientific and technical findings that are preliminary or of specialized interest, e.g., quick release reports, working papers, and bibliographies that contain minimal annotation. Does not contain extensive analysis.

- CONTRACTOR REPORT. Scientific and technical findings by NASA-sponsored contractors and grantees.

- CONFERENCE PUBLICATION. Collected papers from scientific and technical conferences, symposia, seminars, or other meetings sponsored or co-sponsored by NASA.

- SPECIAL PUBLICATION. Scientific, technical, or historical information from NASA programs, projects, and missions, often concerned with subjects having substantial public interest.

- TECHNICAL TRANSLATION. English-language translations of foreign scientific and technical material pertinent to NASA's mission.

Specialized services also include organizing and publishing research results, distributing specialized research announcements and feeds, providing help desk and personal search support, and enabling data exchange services.

For more information about the NASA STI program, see the following:

- Access the NASA STI program home page at *http://www.sti.nasa.gov*

- E-mail your question via the Internet to help@sti.nasa.gov

- Fax your question to the NASA STI Help Desk at 443-757-5803

- Phone the NASA STI Help Desk at 443-757-5802

- Write to:
  NASA STI Help Desk
  NASA Center for AeroSpace Information
  7115 Standard Drive
  Hanover, MD 21076-1320

NASA/TM-2010-216387

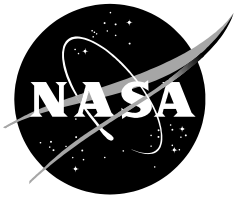

Application of Approximate Unsteady Aerodynamics for Flutter Analysis

Chan-gi Pak and Wesley W. Li
NASA Dryden Flight Research Center
Edwards, California

National Aeronautics and
Space Administration

Dryden Flight Research Center
Edwards, California 93523-0273

July 2010

NOTICE

Use of trade names or names of manufacturers in this document does not constitute an official endorsement of such products or manufacturers, either expressed or implied, by the National Aeronautics and Space Administration.

Available from:

NASA Center for AeroSpace Information
7115 Standard Drive
Hanover, MD 21076-1320
(443) 757-5802

ABSTRACT

A technique for approximating the modal aerodynamic influence coefficient (AIC) matrices by using basis functions has been developed. A process for using the resulting approximated modal AIC matrix in aeroelastic analysis has also been developed. The method requires the unsteady aerodynamics in frequency domain, and this methodology can be applied to the unsteady subsonic, transonic, and supersonic aerodynamics. The flutter solution can be found by the classic methods, such as rational function approximation, k, p-k, p, root locus et cetera. The unsteady aeroelastic analysis using unsteady subsonic aerodynamic approximation is demonstrated herein. The technique presented is shown to offer consistent flutter speed prediction on an aerostructures test wing (ATW) 2 and a hybrid wing body (HWB) type of vehicle configuration with negligible loss in precision. This method computes AICs that are functions of the changing parameters being studied and are generated within minutes of CPU time instead of hours. These results may have practical application in parametric flutter analyses as well as more efficient multidisciplinary design and optimization studies.

NOMENCLATURE

A	general AIC matrix
AIC	aerodynamic influence coefficient
ATW	aerostructures test wing
BFA	basis function approximation
CEM	central executive module
DFRC	Dryden Flight Research Center
g	damping
HWB	hybrid wing body
k	reduced frequency
m	number of mode shapes
MDAO	multidisciplinary design, analysis, and optimization
n	number of basis functions
NASA	National Aeronautics and Space Administration
Q	modal AIC matrix
Q_{ij}	i-th row and j-th column element of the modal AIC matrix Q
$\bar{Q}$	approximate modal AIC matrix
$\bar{Q}_{ij}$	i-th row and j-th column element of the approximate modal AIC matrix $\bar{Q}$
$\tilde{Q}$	basis AIC matrix
$\tilde{Q}_{sr}$	s-th row and r-th column element of the basis AIC matrix $\tilde{Q}$
V	velocity
β_k^i	Modal participation factors of the k-th basis function on the i-th mode shape
β_s^i	Modal participation factors of the s-th basis function on the i-th mode shape
β_k^j	Modal participation factors of the k-th basis function on the j-th mode shape

β_r^j	Modal Participation factors of the r-th basis function on the j-th mode shape
ϕ	mode shape
ϕ_i	i-th mode shape
Φ	modal matrix
Ψ	basis matrix
Ψ_k	k-th basis function
Ψ_r	r-th basis function
Ψ_s^T	s-th transpose of the basis function
ω	frequency

INTRODUCTION

Supporting the Aeronautics Research Mission Directorate guidelines, the National Aeronautics and Space Administration (NASA) Dryden Flight Research Center (DFRC) (Edwards, California) is developing an object-oriented multidisciplinary design, analysis, and optimization (MDAO) tool (ref. 1). This tool will leverage existing tools and practices, and allow the easy integration and adoption of new state-of-the-art software. At the heart of the object-oriented MDAO tool is the central executive module (CEM) as shown in figure 1. In this module, the user will choose an optimization methodology, and provide starting and side constraints for continuous as well as discrete design variables and external file names for interface variables, which communicate between the CEM and each analysis module. The structural analyses modules such as computations of the structural weight, stress, deflection, buckling, and flutter and divergence speeds have been developed and incorporated into the object-oriented MDAO framework.

In general, obtaining aerodynamic influence coefficients (AIC) by direct calculation for integration into preliminary design activities involving disciplines such as aeroelasticity, aeroservoelasticity, and optimization is, at present, a costly and impractical venture (ref. 1). With the increasing complexity of the configuration and the increasing fidelity of the aerodynamic equations, the computational costs increase rapidly. The unsteady aeroelastic analysis and design optimizations are a challenging task. The time required for unsteady computations whether in frequency domain or time domain will considerably slow down the whole design process. Also, these analyses are usually performed repeatedly to optimize the final design. Even though the computational costs may be reduced by the use of advanced algorithms and improved computer hardware processing speeds, these full aeroelasticity analyses cannot be incorporated effectively within a preliminary design and optimization environment. For example, using the ZAERO™ (ZONA Technology Incorporated, Scottsdale, Arizona) code to generate the modal AIC matrix for the IKHANA (a modified Predator® B, General Atomics Aeronautical Systems, Incorporated, San Diego, California) aircraft with existing AIC data, one Mach number, and 16 reduced frequencies, takes an average of 30 min on an Intel® Core™2 2.80 GHz CPU computer (Intel Corporation, Santa Clara, California) (ref. 1). One of the examples presented in this paper, the hybrid wing body (HWB) aircraft, takes about 50 min to generate the modal AICs with existing AIC data.

As a result, there is considerable motivation to be able to perform aeroelastic calculations more quickly and inexpensively using basis function approximation (BFA) method. One of the

primary goals behind the current development is to reduce the computation time for generating modal AIC matrices during the optimization procedure.

BASIS FUNCTION APPROXIMATION

The BFA method requires the unsteady aerodynamics to be represented in the frequency domain. In this study, the BFA for the subsonic and supersonic speeds are discussed. The flutter solution can be found by the classic methods, such as rational function approximation, k, p-k, p, root locus et cetera. A process that efficiently incorporates an approximated modal AIC matrix into the MDAO tool for design optimization at a reasonable computational cost has been developed and is outlined in the flowchart shown in figure 2.

In linear algebra, a basis is a set of vectors that in a linear combination can represent every vector in a given vector space or free module, and no element of the set can be represented as a linear combination of the others (ref. 2). In other words, a basis is a linearly independent spanning set.

This paper discusses an effective approach for approximating a modal AIC matrix for optimization with flutter speed constraints. Consider the steps of the approximation process depicted in the flowchart given in figure 2. Steps 1 and 2 are performed only once before starting the optimization process. Steps 3, 4, and 5 are done iteratively for aeroelasticity calculation.

In step 1, a set of representative basis functions Ψ is defined and intended to capture salient features of the modal responses the airplane is expected to encounter in the design space. Structural mode shapes obtained from different mass or various stiffness configurations of the airplane can be used as the basis functions. These basis functions are comparison functions (ref. 3) since all the geometric and natural boundary conditions of the airplane are satisfied. Each mode shape of the airplane with the target configuration can be approximated as a linear combination of a set of the basis functions. The target configuration in this paper is simply an arbitrary design point within the design space and is used as a check case.

In step 2, the representative basis AIC matrices $\tilde{Q}$ are computed corresponding to the representative basis functions defined in step 1 at any Mach number and reduced frequency. These basis AIC matrices are used as input for approximate modal AIC matrix calculation in step 4.

In step 3, for a set of given design structural mode shapes ϕ, each mode shape is decomposed in a linear combination of the basis functions. The *i*-th target mode shape vector ϕ (*i*=1, 2, …, *m*, where *m* is the number of mode shapes) is approximated through the use of a least squares method of the representative basis functions as shown in equation (1),

$$\phi_i \approx \sum_{k=1}^{n} \beta_k^i \psi_k \tag{1}$$

where a vector ψ_k is the k-th basis function and a scalar coefficient β_k^i is the modal participation factor of the k-th basis function on the i-th mode shape; n is the number of basis functions.

In step 4, an approximate modal AIC matrix $\bar{Q}$ is computed based on a basis AIC matrix $\tilde{Q}$ and modal participation factors. Let matrices Q, A, and Φ be a modal AIC matrix, a general AIC matrix, and a modal matrix, respectively. Then the modal AIC matrix Q can be defined as shown in equation (2),

$$Q = \Phi^T A \Phi$$

$$\text{where } \Phi = [\phi_1 \ \phi_2 \cdots \phi_m] \tag{2}$$

Therefore the i-th row and j-th column element of the modal AIC matrix Q can be written as shown in equation (3),

$$Q_{ij} = \phi_i^T A \phi_j \tag{3}$$

Substituting equation (1) into equation (3) is given in equation (4),

$$Q_{ij} = \phi_i^T A \phi_j \approx \left(\sum_{k=1}^{n} \beta_k^i \psi_k^T \right) A \left(\sum_{k=1}^{n} \beta_k^j \psi_k \right) = \bar{Q}_{ij}$$

$$\bar{Q}_{ij} = \sum_{r=1}^{n} \sum_{s=1}^{n} \beta_s^i \beta_r^j \psi_s^T A \psi_r \tag{4}$$

The detailed derivations of equation (4) are listed in Appendix A. Let the basis AIC matrix $\tilde{Q}$ be defined as shown in equation (5),

$$\tilde{Q} = \Psi^T A \Psi \tag{5}$$

then the *s*-th row and *r*-th column element of the $\tilde{Q}$ can be written as shown in equation (6),

$$\tilde{Q}_{sr} = \psi_s^T A \psi_r \tag{6}$$

Substituting equation (6) into equation (4) gives equation (7) for the approximate modal AIC matrix.

$$\bar{Q}_{ij} = \sum_{r=1}^{n} \sum_{s=1}^{n} \beta_s^i \beta_r^j \tilde{Q}_{sr} \tag{7}$$

The basis AIC matrix $\tilde{Q}$ in equation (5) can be computed and saved before starting optimization as mentioned in step 2. During optimization, the mode shapes, ϕ_i (i=1, 2, …, m), are fitted using basis functions ψ_k and modal participation factors β_k^i as shown in equation (1), and the approximate modal AIC matrix $\bar{Q}$ can be computed using equation (7). This approximate modal AIC matrix will be used for flutter analysis in step 5. The resulting flutter speed and frequency could be used for optimization. In step 5, the flutter solution can be found by the classic methods, such as rational function approximation, k, p-k, p, root locus et cetera.

APPLICATIONS

In order to validate the proposed BFA technique in subsonic flight regimes, the flutter results using this approximate method are compared with the direct flutter results. First a simple model from the aerostructures test wing (ATW) 2 program was chosen. Subsequently, a complex practical problem HWB model was analyzed. In this study, structural mode shapes obtained from different mass configurations of the airplane are used as basis functions.

A Modified Aerostructures Test Wing 2

The proposed technique has been applied and validated using a modified ATW2. The original ATW2 (ref. 4) test article was actually designed, built, and flight-tested at NASA DFRC as shown in figure 3. This wing was cantilevered from a center station pylon and flown on the McDonnell Douglas (now The Boeing Company, Chicago, Illinois) NF-15B test bed aircraft.

In this study, calculated structural mode shapes obtained from different mass configurations of the wing are used as basis functions. To create each different mass configuration, the mass at each mass point is represented using an additional concentrated mass element attached through rigid body elements to the finite element model as shown in figure 4. These alterations unintentionally increased the effective wing stiffness and the first natural frequency over that of the actual ATW2 configuration (ref. 5) in spite of the mass increase because of the rigid elements.

The total weight and center of gravity of the various fictitious and target ATW2 mass configurations are listed in table 1. The direct flutter analysis of the target configuration (mass = 0.0 units) is performed at Mach 0.82 with 16 reduced frequencies using MSC/NASTRAN (MSC

Software Corporation, Santa Ana, California) and ZAERO™ codes (refs. 6-7). In order to have better flutter solution convergence for flutter speed, the first 10 structural modes are included in the calculation. While preparing for the approximate flutter solution, three different mass configurations, 0.3, 0.6, and 0.9 units were selected for generating the basis functions.

In order to be able to capture more of the target mode shapes, larger basis functions were generated. Fifteen structural mode shapes for each mass configuration were generated using MSC/NASTRAN. The natural frequencies of the various fictitious and target ATW2 mass configurations are listed in table 2. According to Pak and Lung (ref. 5), the primary natural modes for the first flutter mode are mode numbers 1, 2, and 3; and all of the higher modes are the secondary modes. The first three natural frequencies and mode shapes are the first bending, the first torsion, and the second bending modes, respectively and are shown in figure 5. A total of 45 basis functions were generated. Then the 45 by 45 basis AIC matrix corresponding to those 45 basis functions was computed for each of 16 reduced frequencies at Mach 0.82 using ZAERO™. The mode shapes of the target configuration are fitted using the basis functions together with a least squares method; and then the approximate modal AIC matrices were computed, and the flutter analysis was performed.

For the present test case, ATW2 mode shapes, generated from direct method and BFA method, are plotted in figures 5a, 5b, and 5c. The approximated mode shapes are very well matched to the target mode shapes. The difference of the first three mode shapes between these two methods is plotted in figure 6.

The results of the matched flutter analysis using the direct method and the BFA method are summarized in table 3. Three percent damping was used for the flutter speed and frequency computation. Both methods predicted the same flutter speed of 543.59 KEAS at a flutter frequency of 49.01 Hz. The speed versus damping, V-g, and speed versus frequency, V-ω curves from the direct and BFA methods at Mach 0.82 are given in figures 7 and 8.

Table 4 lists the computational cost of computing the modal AIC with a given structural mode shape at one Mach number using the direct method and the BFA method. The comparison was done on an Intel® Core™2 2.80 GHz CPU computer. The computational cost of generating the basis functions before the parametric study is not included in the comparison.

Hybrid Wing Body Vehicle

The modified ATW2 is a simple cantilevered wing model and a straight forward application. A hybrid wing body (HWB) aircraft (ref. 8) was selected for a second and more challenging demonstration of the BFA method.

In this HWB application, the basis functions are created based on three different total fuel conditions of the vehicle, configuration number 1, 2, and 3. The target model weight is bounded by the range of the weight of configurations 2 and 3. In the finite element model, the various fuel weights are modeled using a concentrated mass element attached directly to each of the node points in the fuel tank area as shown in figure 9 (ref. 9). The total weight and center of gravity location of the different fuel weight and target configurations are listed in table 5.

With target configuration, the direct flutter analysis is performed at Mach 0.50, with 40 structural modes and 14 reduced frequencies using MSC/NASTRAN and ZAERO™ codes. A classical wing bending torsion type of flutter was predicted in this HWB example. The first fourteen flexible natural frequencies and the first four flexible mode shapes are listed in table 6

and figure 10, respectively. The first four modes are the first symmetric and anti-symmetric bending, and the first symmetric and anti-symmetric torsion.

For the approximate flutter solution, a total of 150 basis functions are generated from 3 different fuel configurations and 50 structural mode shapes for each fuel configuration using MSC/NASTRAN. Then the 150 by 150 basis AIC matrix corresponding to those 150 basis functions is computed for each of 14 reduced frequencies at Mach 0.50 using ZAERO™.

The flutter boundary of the HWB at Mach 0.50 using BFA method is compared to that from the direct method. The flutter boundaries are summarized in table 7. The flutter speed is normalized with respect to direct method flutter speed. With 3-percent structural damping, the normalized flutter speed using the BFA method is 0.991, and the flutter frequency is 2.671 Hz. The percentage errors of the flutter speed and frequency are 0.86 percent and 0.15 percent. The speed versus damping, V-g, and the speed versus frequency, V-ω, curves of the HWB at Mach 0.50 obtained from the direct and BFA methods are given in figures. 11 and 12. The BFA offers consistent flutter speed and frequency predictions on the HWB target configuration. See table 4 for the computational cost of the HWB example. The computational cost of generating the basis functions and AIC is about 250 min in this HWB example.

CONCLUSION

A technique for approximating the modal AIC matrix by using basis functions has been developed and validated, and a process for using the resulting AIC matrix in aeroelastic analysis and design optimization has been proposed. The approximation method has been applied to the aeroelastic analyses, and the results are essentially identical to those using direct solution. The technique presented has been shown to offer consistent flutter speed prediction on an ATW2 configuration and a HWB type vehicle with a negligibly small loss in precision. These results may have practical significance in the analysis of aircraft aeroelastic calculation and could lead to a more efficient design optimization cycle. The basis function approximation approach yields significant improvements in computational efficiency as compared to the original approach, thereby meeting the objective of this study.

TABLES

Table 1. Summary of total weight and center of gravity location for the ATW2 with different fictitious mass configurations.

Mass configuration	1	2	3	Target
Total weight, lb	4.046	5.250	6.450	2.850
X center of gravity, in	14.510	14.950	15.220	13.710
Y center of gravity, in	-8.760	-9.010	-9.170	-8.290
Z center of gravity, in	0.000	0.000	0.000	0.000
Number of modes	15	15	15	10

Table 2. Summary of natural frequencies (Hz) of the ATW2 with different fictitious mass configurations.

Mode	Configuration 1	Configuration 2	Configuration 3	Target
1	18.10	15.98	14.45	21.32
2	62.81	61.91	60.60	63.55
3	85.87	77.10	71.84	103.18
4	126.60	112.29	101.86	147.79
5	191.68	173.89	160.47	208.55
6	230.10	220.25	215.18	265.53
7	357.83	317.80	290.89	408.75
8	403.33	383.13	367.52	434.86
9	450.24	444.21	426.69	472.85
10	532.04	477.94	448.37	589.94
11	628.72	616.37	600.44	
12	633.07	630.08	628.51	
13	708.57	707.15	684.02	
14	729.18	726.37	705.74	
15	782.46	728.68	725.76	

Table 3. Summary of the ATW2 flutter results comparison for BFA and direct method.

	BFA method	Direct method	Error, %
Flutter speed, KEAS	543.59	543.59	0.0
Flutter frequency, Hz	49.01	49.01	0.0

Table 4. Computational cost comparison of BFA and direct method.

Test case	ATW2	HWB
Number of nodes	269	~24000
Number of structural modes	10	40
Number of reduced frequencies	16	14
Direct method elapsed time	43 s	50 min
BFA method elapsed time	8 s	9 min

Table 5. Different fuel weight configurations versus target fuel weight configurations of the HWB.

Mass configuration	1	2	3	Target
Total weight, lb	403781	478941	591681	535311
X center of gravity, in	1337.60	1334.51	1331.34	1332.76
Y center of gravity, in	0.75	0.46	0.16	0.29
Z center of gravity, in	20.89	21.35	21.82	21.61
Number of modes	50	50	50	40

Table 6. Natural frequencies (Hz) of the HWB with various fuel weight and target fuel weight configurations.

Mode	Configuration 1	Configuration 2	Configuration 3	Target
1	1.60	1.54	1.47	1.50
2	1.74	1.64	1.53	1.58
3	3.52	3.35	3.13	3.24
4	3.64	3.45	3.22	3.33
5	5.24	5.00	4.54	4.83
6	5.26	5.04	4.54	4.89
7	6.42	5.42	4.68	4.92
8	6.42	5.43	4.76	4.92
9	6.92	6.66	5.81	6.31
10	7.12	6.68	5.82	6.31
11	7.33	6.95	6.11	6.39
12	7.65	6.95	6.32	6.48
13	8.22	7.03	6.69	6.85
14	8.23	7.40	7.06	7.22

Table 7. Summary of the HWB flutter results comparison for BFA and direct method.

	BFA method	Direct method	Error, %
Flutter speed, normalized	0.991	1.000	0.86
Flutter frequency, Hz	2.671	2.667	0.15

FIGURES

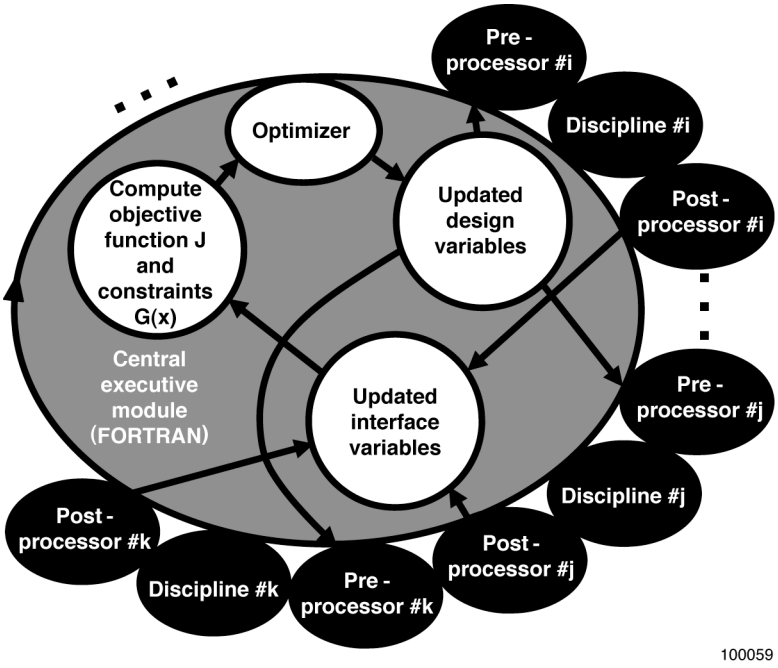

Figure 1. Object-oriented multidisciplinary design, analysis, and optimization tool.

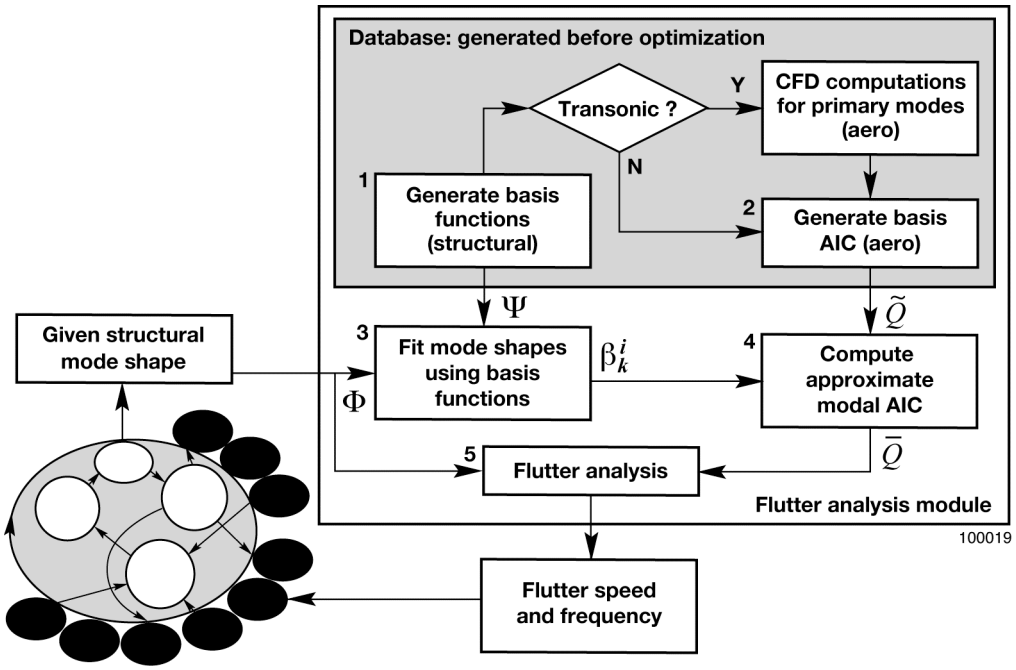

Figure 2. Flowchart of the flutter analysis module in object-oriented MDAO tool.

Figure 3. Aerostructures test wing 2.

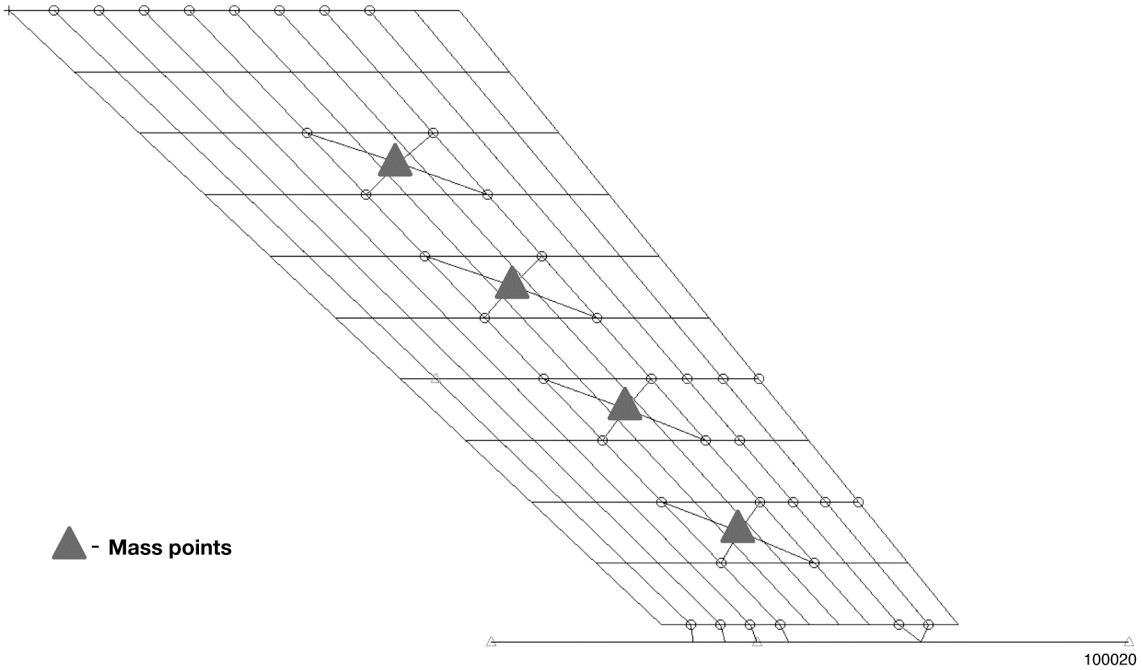

Figure 4. Aerostructures test wing 2 finite element model with fictitious mass point locations.

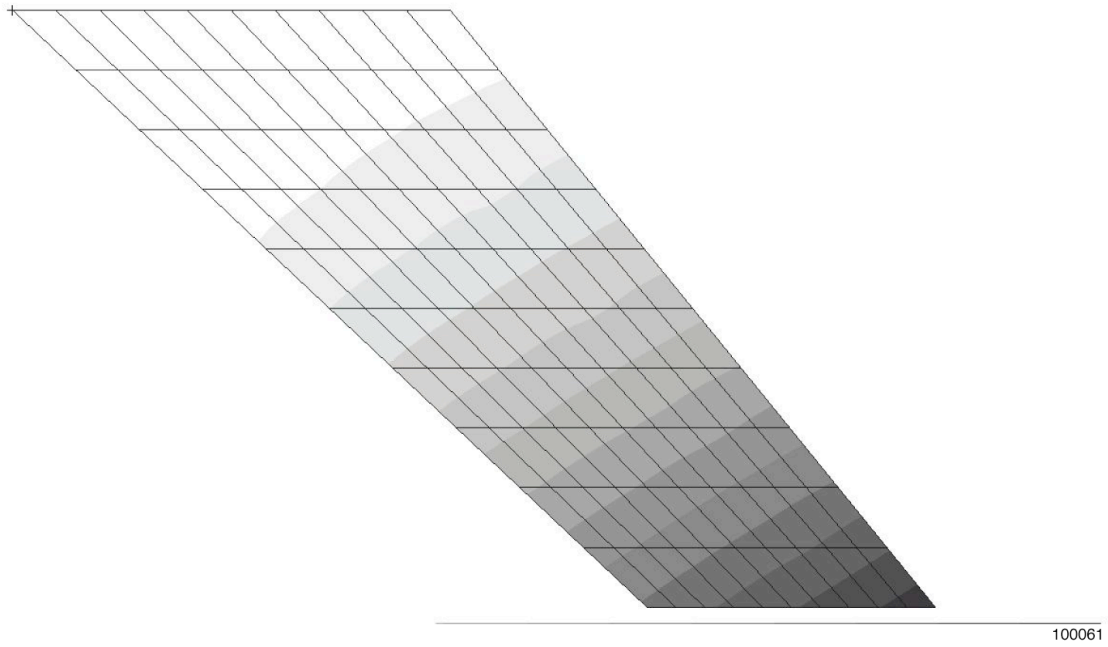

Figure 5a. Mode 1 (First bending), 21.32 Hz.

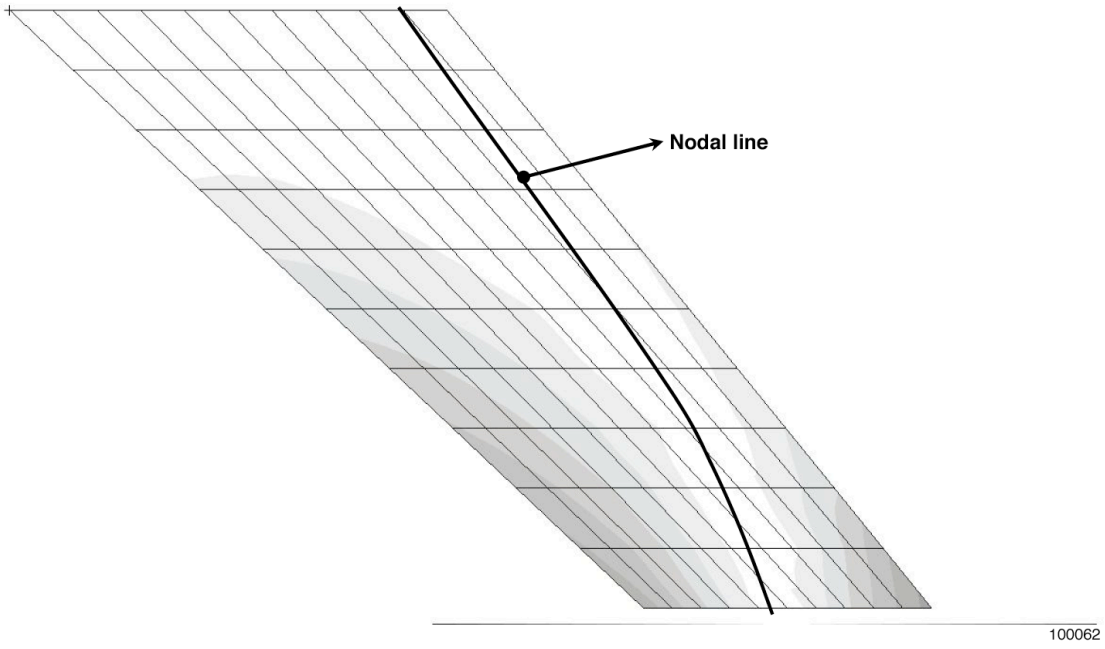

Figure 5b. Mode 2 (Second bending and first torsion), 63.55 Hz.

Figure 5. Structural finite element model mode shapes and frequencies of the ATW2 with target mass configuration (direct method).

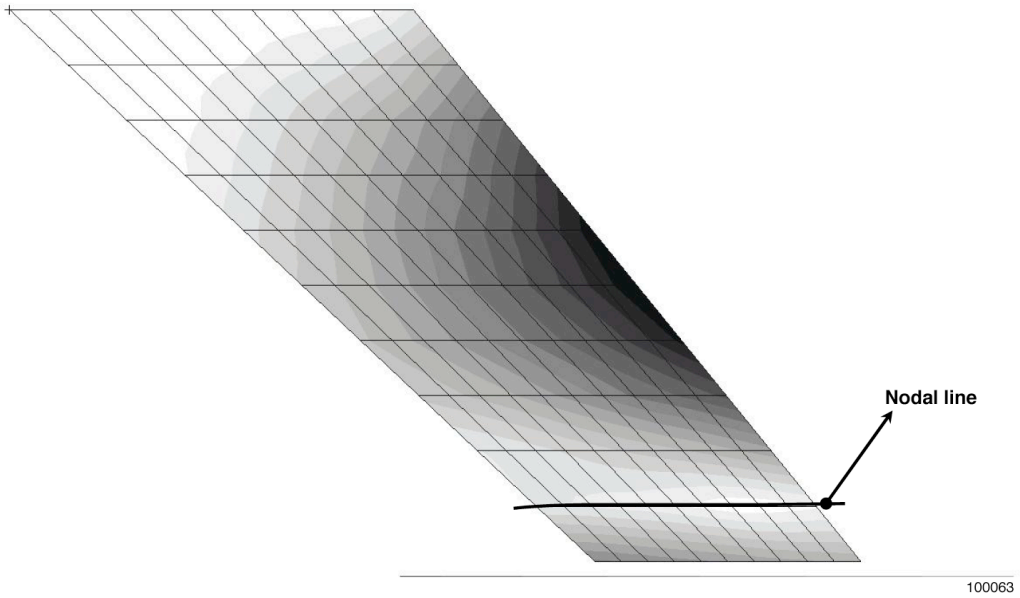

Figure 5c. Mode 3 (Second bending and first torsion), 103.18 Hz.

Figure 5. Concluded.

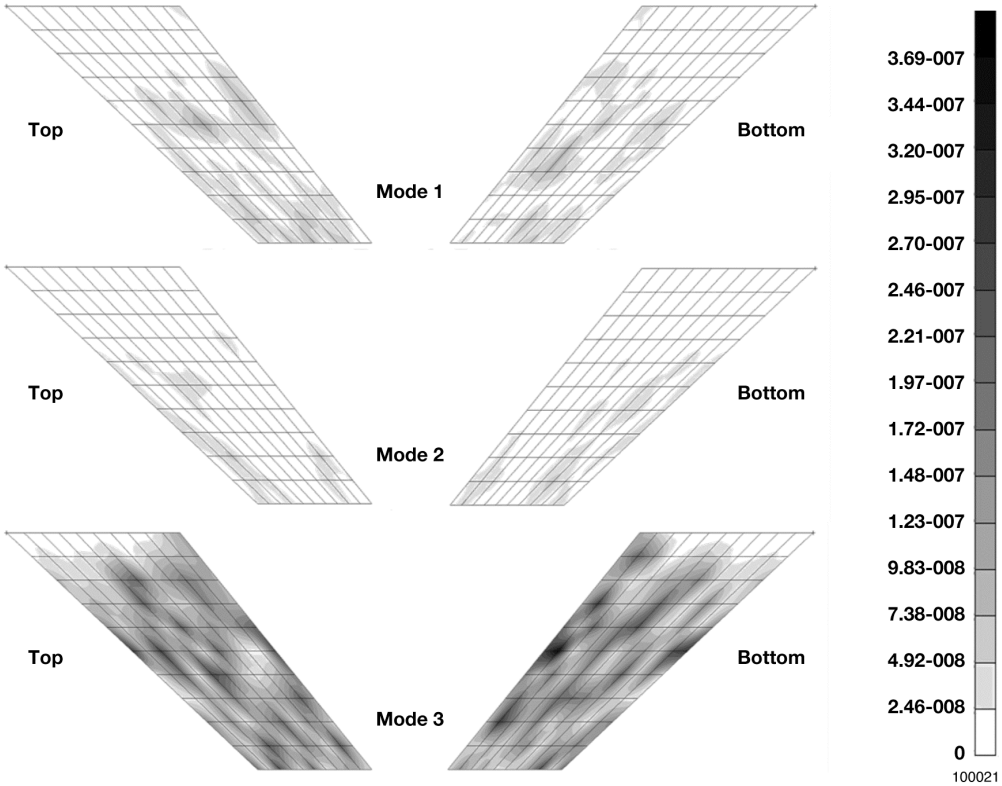

Figure 6. Structural finite element model mode shapes error of the ATW2 with target mass configuration.

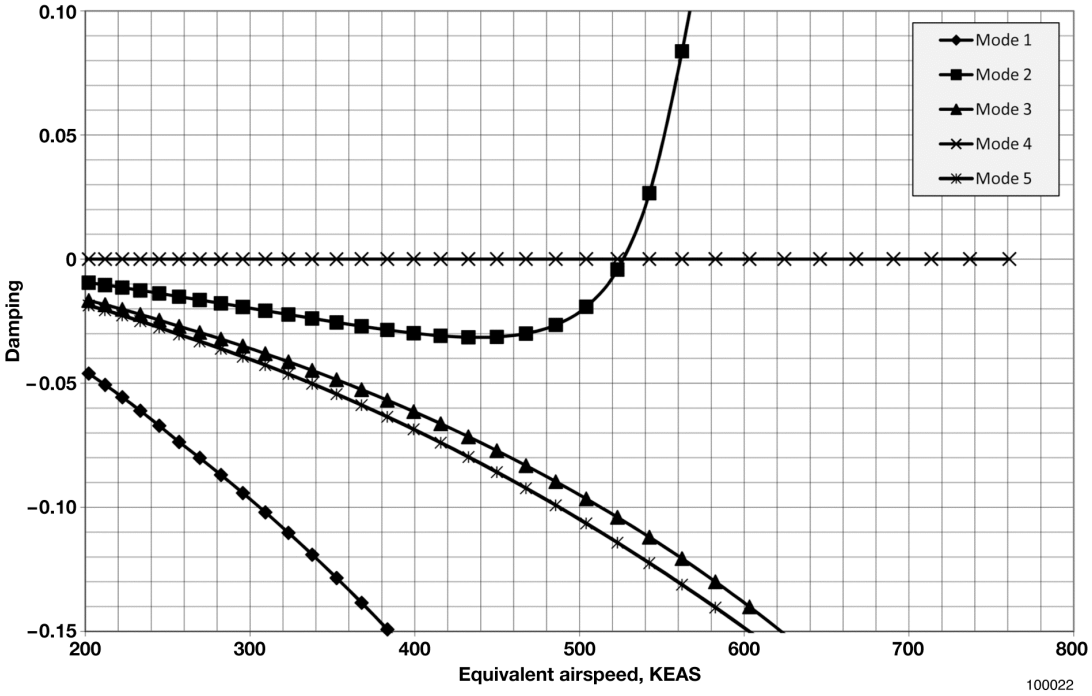

Figure 7a. V-g plot.

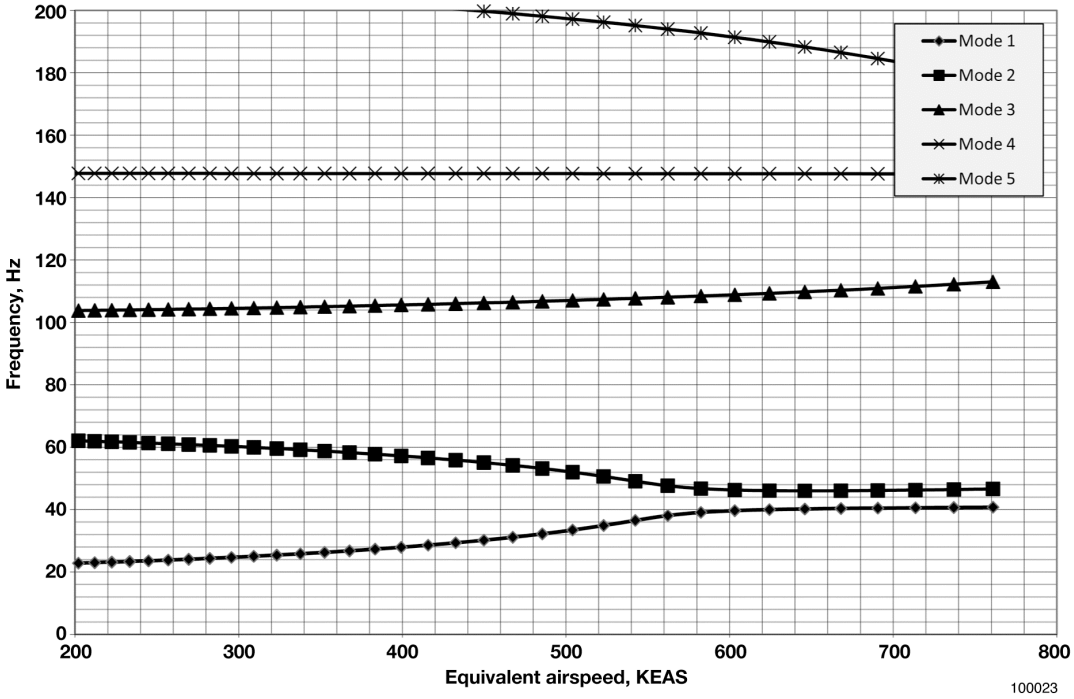

Figure 7b. V-ω plot.

Figure 7. V-g and V-ω plots for the ATW2 at Mach 0.82 using direct modal AIC matrices.

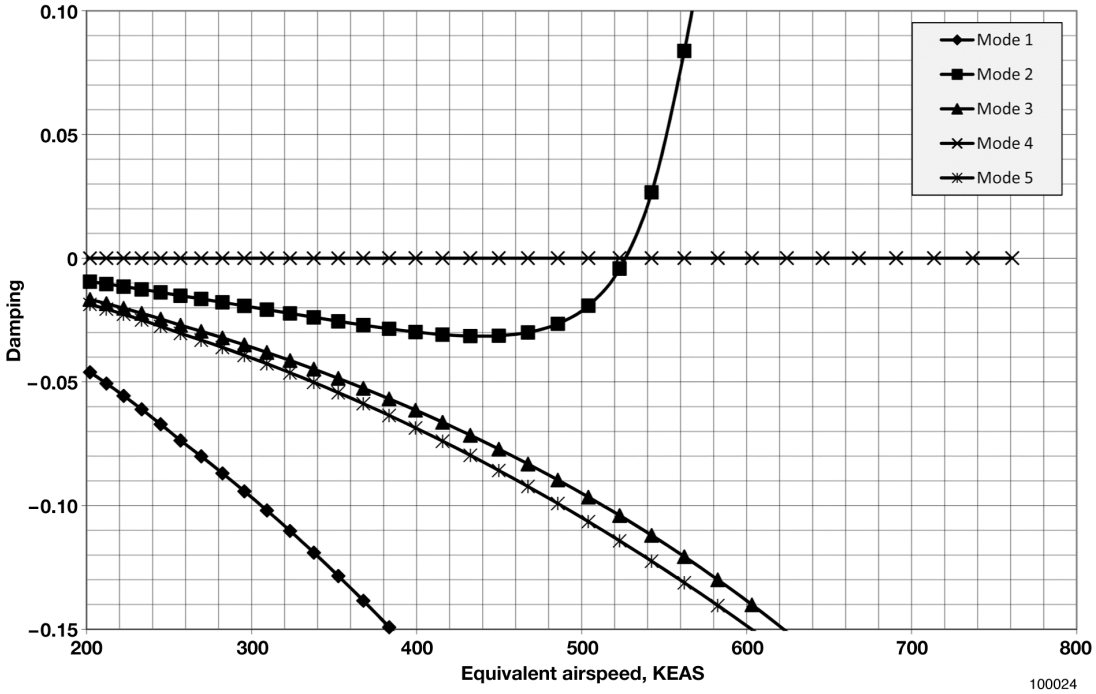

Figure 8a. V-g plot.

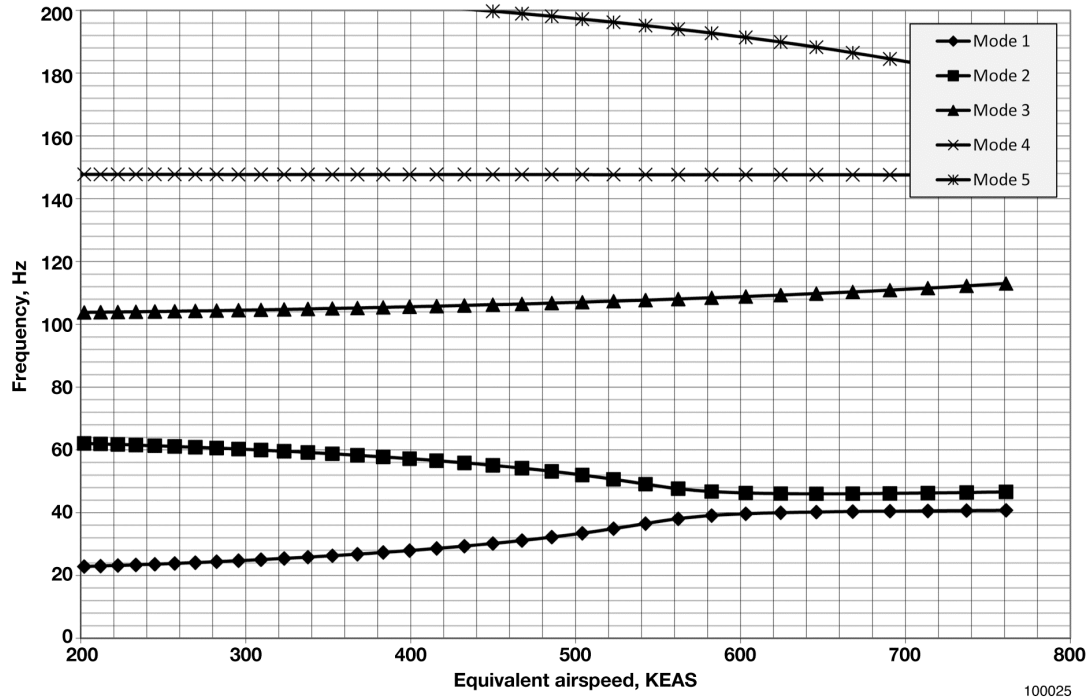

Figure 8b. V-ω plot.

Figure 8. V-g and V-ω plots for the ATW2 at Mach 0.82 using approximate modal AIC matrices.

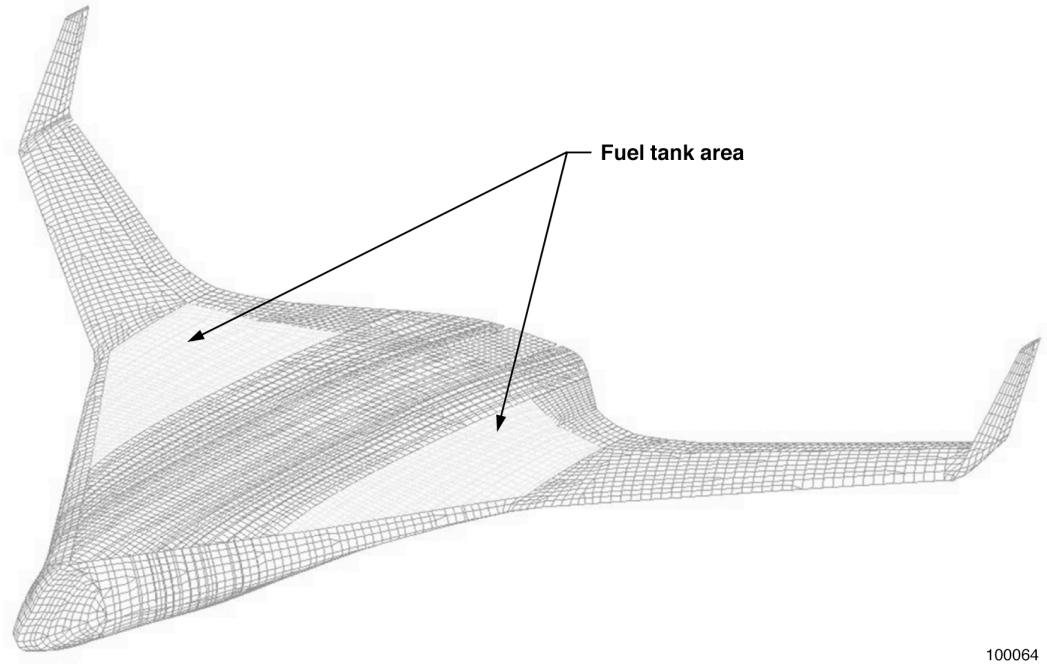

Figure 9. Hybrid wing body aircraft finite element model.

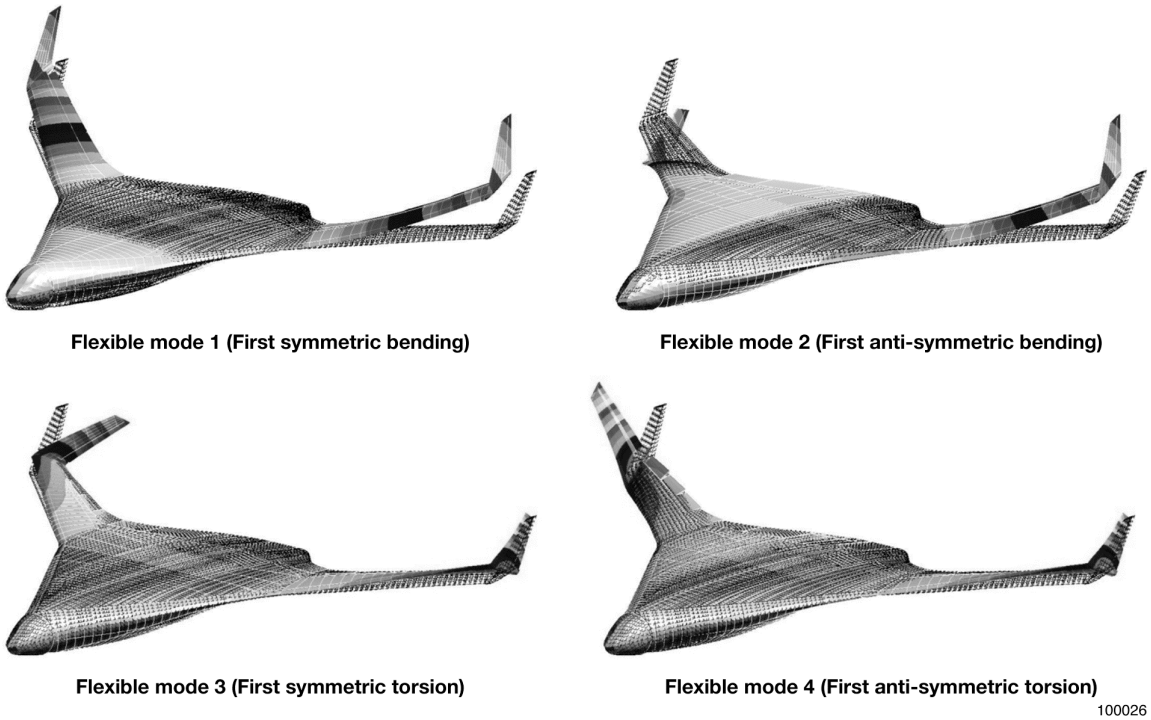

Figure 10. Hybrid wing body mode shapes.

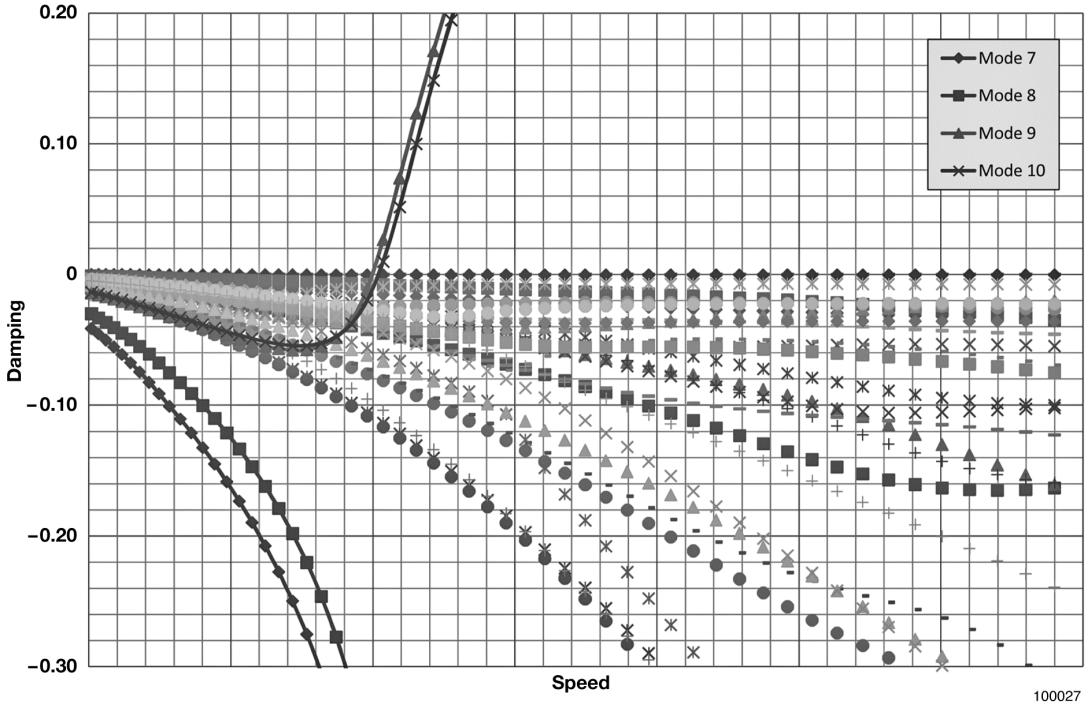

Figure 11a. V-g plot.

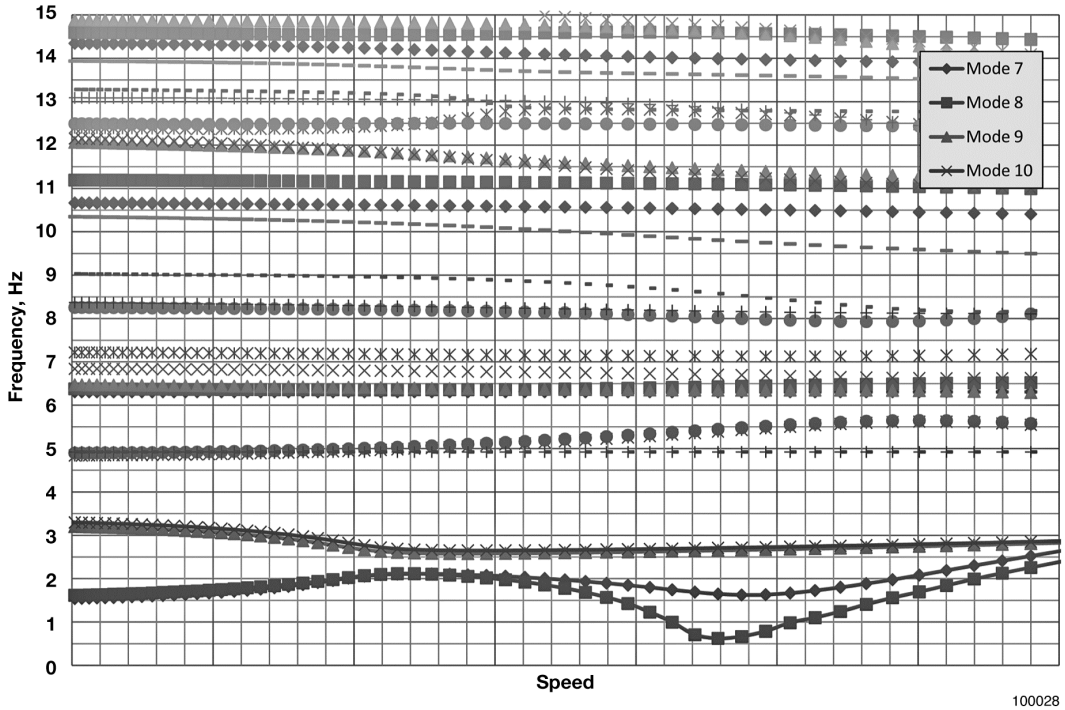

Figure 11b. V-ω plot.

Figure 11. V-g and V-ω plots for the HWB at Mach 0.50 using direct modal AIC matrices.

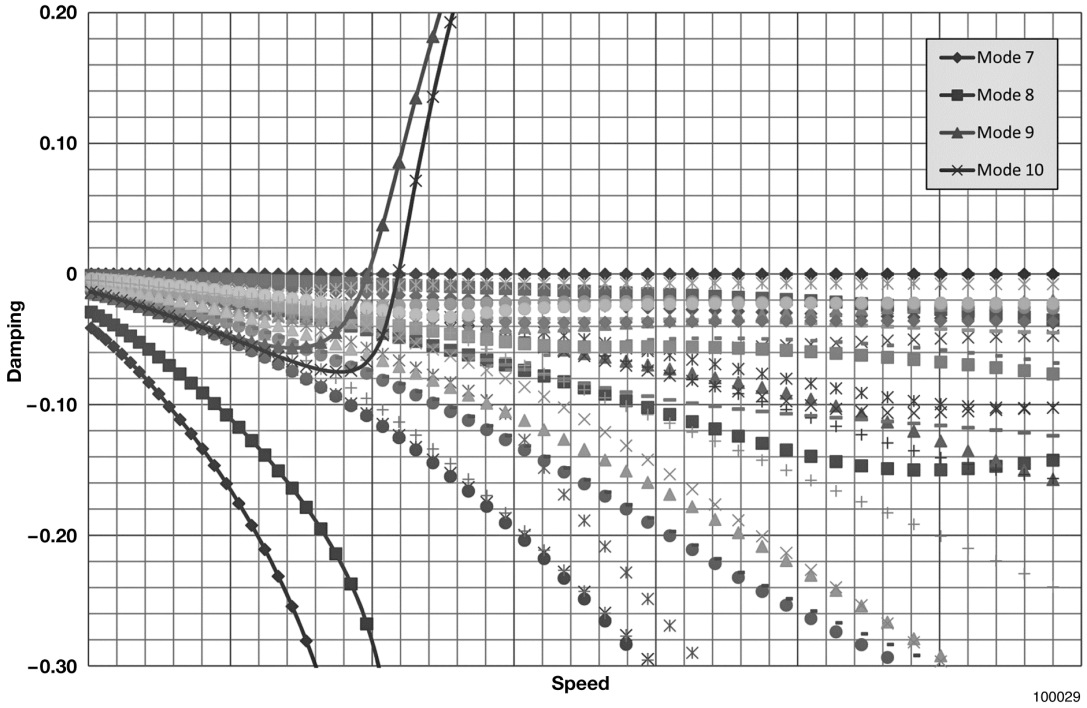

Figure 12a. V-g plot.

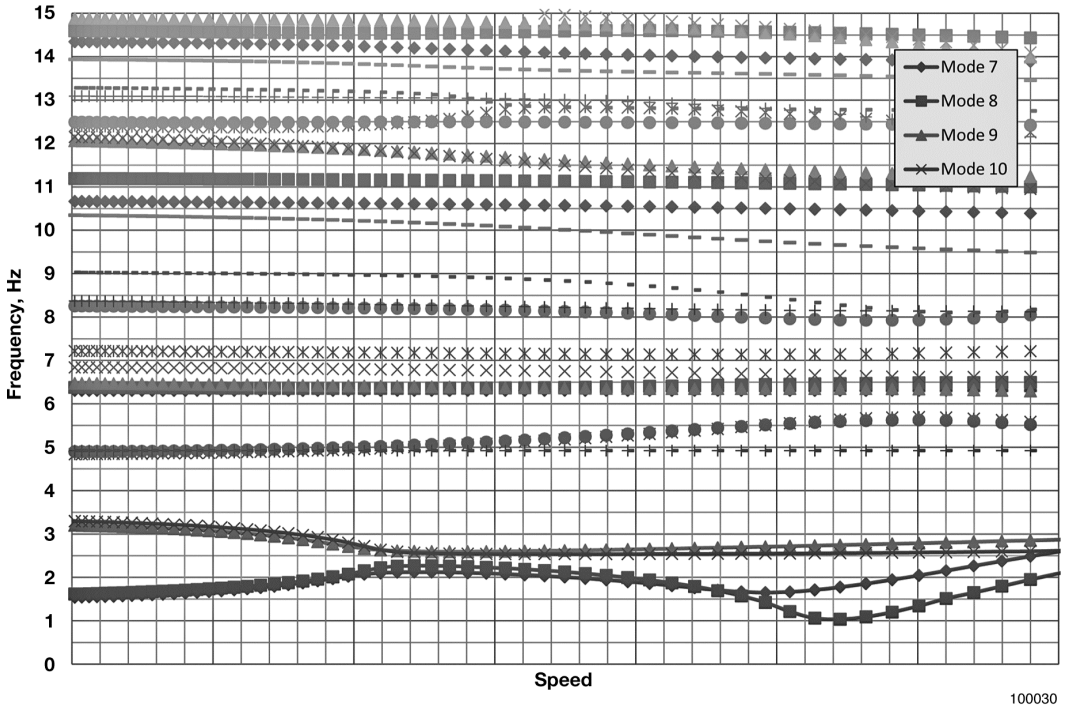

Figure 12b. V-ω plot.

Figure 12. V-g and V-ω plots for the HWB at Mach 0.50 using approximate modal AIC matrices.

APPENDIX A
BASIS FUNCTION APPROXIMATION

$$\overline{Q}_{ij} = \left(\sum_{k=1}^{n} \beta_k^i \psi_k^T \right) A \left(\sum_{k=1}^{n} \beta_k^j \psi_k \right)$$

$$= \left(\sum_{k=1}^{n} \beta_k^i \psi_k^T \right) A \left(\beta_1^j \psi_1 + \beta_2^j \psi_2 + \cdots + \beta_n^j \psi_n \right)$$

$$= \left(\sum_{k=1}^{n} \beta_k^i \psi_k^T \right) \left(A\beta_1^j \psi_1 + A\beta_2^j \psi_2 + \cdots + A\beta_n^j \psi_n \right)$$

$$= \left(\sum_{k=1}^{n} \beta_k^i \psi_k^T \right) \left(\beta_1^j A\psi_1 + \beta_2^j A\psi_2 + \cdots + \beta_n^j A\psi_n \right)$$

$$= \left(\beta_1^i \psi_1^T + \beta_2^i \psi_2^T + \cdots + \beta_n^i \psi_n^T \right) \left(\beta_1^j A\psi_1 + \beta_2^j A\psi_2 + \cdots + \beta_n^j A\psi_n \right)$$

$$= \beta_1^i \psi_1^T \beta_1^j A\psi_1 + \beta_2^i \psi_2^T \beta_1^j A\psi_1 + \cdots + \beta_n^i \psi_n^T \beta_1^j A\psi_1$$

$$+ \beta_1^i \psi_1^T \beta_2^j A\psi_2 + \beta_2^i \psi_2^T \beta_2^j A\psi_2 + \cdots + \beta_n^i \psi_n^T \beta_2^j A\psi_2 + \cdots +$$

$$+ \beta_1^i \psi_1^T \beta_n^j A\psi_n + \beta_2^i \psi_2^T \beta_n^j A\psi_n + \cdots + \beta_n^i \psi_n^T \beta_n^j A\psi_n$$

$$= \beta_1^i \beta_1^j \psi_1^T A\psi_1 + \beta_2^i \beta_1^j \psi_2^T A\psi_1 + \cdots + \beta_n^i \beta_1^j \psi_n^T A\psi_1$$

$$+ \beta_1^i \beta_2^j \psi_1^T A\psi_2 + \beta_2^i \beta_2^j \psi_2^T A\psi_2 + \cdots + \beta_n^i \beta_2^j \psi_n^T A\psi_2 + \cdots +$$

$$+ \beta_1^i \beta_n^j \psi_1^T A\psi_n + \beta_2^i \beta_n^j \psi_2^T A\psi_n + \cdots + \beta_n^i \beta_n^j \psi_n^T A\psi_n$$

$$= \beta_1^i \beta_1^j \psi_1^T A\psi_1 + \beta_1^i \beta_2^j \psi_1^T A\psi_2 + \cdots + \beta_1^i \beta_n^j \psi_1^T A\psi_n$$

$$+ \beta_2^i \beta_1^j \psi_2^T A\psi_1 + \beta_2^i \beta_2^j \psi_2^T A\psi_2 + \cdots + \beta_2^i \beta_n^j \psi_2^T A\psi_n + \cdots +$$

$$+ \beta_n^i \beta_1^j \psi_n^T A\psi_1 + \beta_n^i \beta_2^j \psi_n^T A\psi_2 + \cdots + \beta_n^i \beta_n^j \psi_n^T A\psi_n$$

$$\overline{Q}_{ij} = \sum_{r=1}^{n} \sum_{s=1}^{n} \beta_s^i \beta_r^j \psi_s^T A\psi_r \qquad \text{(A1)}$$

REFERENCES

1. Pak, Chan-gi, and Wesley Li, "Multidisciplinary Design, Analysis and Optimization Tool Development Using a Genetic Algorithm," *Proceedings of the 26th Congress of International Council of the Aeronautical Sciences*, Anchorage, Alaska, 2008.

2. Kahaner, David, Cleve Moler, and Stephen Nash, *Numerical Methods and Software*, Prentice-Hall, Englewood Cliffs, New Jersey, 1989.

3. Meirovitch, Leonard, *Analytical Methods in Vibrations*, Macmillan Series in Applied Mechanics, The Macmillan Company, New York, 1967.

4. Lung, Shun-fat, and Chan-gi Pak, "Updating the Finite Element Model of the Aerostructures Test Wing Using Ground Vibration Test Data," AIAA-2009-2528, *Proceedings of the 50th AIAA/ASME/ASCE/AHS/ASC Structures, Structural Dynamics, and Materials Conference*, Palm Springs, California, 2009.

5. Pak, Chan-gi, and Shun-fat Lung, "Reduced Uncertainties in the Robust Flutter Analysis of the Aerostructures Test Wing," *Proceedings of the 27th Congress of International Council of the Aeronautical Sciences*, Nice, France, 2010 (to be published).

6. *ZAERO Theoretical Manual*, ZONA Technology, Incorporated, 2007.

7. *MSC/NASTRAN 2004 Quick Reference Guide*, MSC.Software Corporation, Santa Ana, California, 2004.

8. Felder, James L., Hyun Dae Kim, and Gerald V. Brown, "Turboelectric Distributed Propulsion Engine Cycle Analysis for Hybrid-Wing-Body Aircraft," AIAA-2009-1132, *Proceedings of the 47th AIAA Aerospace Sciences Meeting*, Orlando, Florida, 2009.

9. Velicki, Alex, "Damage Arresting Composites for Shaped Vehicles - Phase 1 Final Report," NASA/CR-2009-215932, 2009.

REPORT DOCUMENTATION PAGE

Form Approved
OMB No. 0704-0188

1. REPORT DATE *(DD-MM-YYYY)*	2. REPORT TYPE	3. DATES COVERED *(From - To)*
01-07-2010	Technical Memorandum	

4. TITLE AND SUBTITLE
Application of Approximate Unsteady Aerodynamics for Flutter Analysis

5a. CONTRACT NUMBER

5b. GRANT NUMBER

5c. PROGRAM ELEMENT NUMBER

6. AUTHOR(S)
Chan-gi Pak and Wesley W. Li

5d. PROJECT NUMBER

5e. TASK NUMBER

5f. WORK UNIT NUMBER

7. PERFORMING ORGANIZATION NAME(S) AND ADDRESS(ES)
NASA Dryden Flight Research Center
P.O. Box 273
Edwards, California 93523-0273

8. PERFORMING ORGANIZATION REPORT NUMBER
H-3058

9. SPONSORING/MONITORING AGENCY NAME(S) AND ADDRESS(ES)
National Aeronautics and Space Administration
Washington, DC 20546-0001

10. SPONSORING/MONITOR'S ACRONYM(S)
NASA

11. SPONSORING/MONITORING REPORT NUMBER
NASA/TM-2010-216387

12. DISTRIBUTION/AVAILABILITY STATEMENT
Unclassified -- Unlimited
Subject Category 02 Availability: NASA CASI (443) 757-5802 Distribution: Standard

13. SUPPLEMENTARY NOTES
Pak and Li, NASA Dryden Flight Research Center. Also presented as AIAA-2010-3085 at the 51st AIAA/ASME/ASCE/AHS/ASC Structures, Structural Dynamics, and Materials Conference, Orlando, Florida, April 12-15, 2010.

14. ABSTRACT

A technique for approximating the modal aerodynamic influence coefficient (AIC) matrices by using basis functions has been developed. A process for using the resulting approximated modal AIC matrix in aeroelastic analysis has also been developed. The method requires the unsteady aerodynamics in frequency domain, and this methodology can be applied to the unsteady subsonic, transonic, and supersonic aerodynamics. The flutter solution can be found by the classic methods, such as rational function approximation, k, p-k, p, root locus et cetera. The unsteady aeroelastic analysis using unsteady subsonic aerodynamic approximation is demonstrated herein. The technique presented is shown to offer consistent flutter speed prediction on an aerostructures test wing (ATW) 2 and a hybrid wing body (HWB) type of vehicle configuration with negligible loss in precision. This method computes AICs that are functions of the changing parameters being studied and are generated within minutes of CPU time instead of hours. These results may have practical application in parametric flutter analyses as well as more efficient multidisciplinary design and optimization studies.

15. SUBJECT TERMS
Aerodynamics influence coefficient matrix, Basis function approximation, Flutter analysis, Least squares method, Multidisciplinary design optimization

16. SECURITY CLASSIFICATION OF:			17. LIMITATION OF ABSTRACT	18. NUMBER OF PAGES	19b. NAME OF RESPONSIBLE PERSON
a. REPORT	b. ABSTRACT	c. THIS PAGE			STI Help Desk (email: help@sti.nasa.gov)
					19b. TELEPHONE NUMBER *(Include area code)*
U	U	U	UU	25	(443) 757-5802